Theoretical and Experimental Investigations on Multiple Pure Tone Noise

R. A. KANTOLA* AND M. KUROSAKA†
General Electric Research and Development Center, Schenectady, N.Y.

An investigation on multiple pure tone (MPT) noise is described. Experiments conducted on a model fan, operating in a closed loop acoustical facility (filled with Freon 12), have revealed that the MPT noise level decreases at the higher rotor Mach numbers. This trend is influenced by the inlet duct length, with the shorter inlet having an earlier peak in the MPT level. The blade nonuniformities are measures and the evolution of the total sound spectra is computed using a previous analysis. The analysis correctly predicts both the frequency and the level of the dominant multiple pure tones. Also, the blade passing frequency noise predictions are in good agreement with the experimental data. From these comparisons it is concluded that a two dimensional, inviscid analysis is adequate to describe the essential features of the MPT noise evolution.

Introduction

In recent years the reduction of jet engine noise has been dramatic. These improvements have largely been concentrated on the blade passing frequencies and their higher harmonics. The contributions of these components have been so reduced that attention is now being focused on the next most objectionable sound emanating from the jet engine, that is, the multiple pure tone sound. In the frequency spectrum measured in the forward arc of an engine, multiple pure tone sounds appear as discrete frequency noise. Their frequencies are integer multiples of the shaft frequency.

In a paper by one of the authors,[1] the theoretical analysis of multiple pure tone sound (MPT) is discussed. In this previous paper it is argued that the MPT originates as the irregular propagation of bow shocks emanating from the leading edge of blades. The irregularities result from blade-to-blade nonuniformities. An analysis is presented under the assumption that the bow shock waves are attached. The flowfield is approximated by an inviscid, two-dimensional model. From the sample calculation, based on nonuniformities within the manufacturing tolerances, it was concluded that such defects are a likely cause of the MPT noise. Particularly significant is the influence of the nonuniformities in the stagger angle. The computed results, based on stagger errors, show that it takes only a few blade spacings ahead of the rotor for the MPT noise to evolve. This trend agrees with the previous observations.

Presented here is the experimental phase of multiple pure tone noise investigations and its comparison with the theory. This study is based on the results of Ref. 2.

The specific objectives of the present investigation are as follows: 1) first, to compare the theoretical predictions, based on Ref. 1, with the experimental results. 2) second, to determine the effect of the relative Mach number and the flow angle on the evolution of the MPT sound. 3) third, to determine the effect of the inlet duct length on the MPT sound generation.

Previous investigators[3-5] have studied the growth of the multiple pure tones in full-sized compressors. In most of these cases the flow geometry upstream of the rotor plane was rapidly diverging, i.e., an inlet bellmouth was used. Only a limited amount of data[4] was taken in a constant area annulus. In this investigation, to establish the connection between blade defects and the MPT generation, the rotor nonuniformities are measured and used to predict the MPT generation. To allow a reasonably valid comparison between the predictions and experiments a constant area inlet annulus of approximately nine rotor blade spacings is used. The evolution of the wave pattern in this long inlet is investigated by placing piezo-electric pressure transducers in the outer wall at three upstream locations. Measurements of the noise emanating from the compressor inlet are taken by a traversing microphone in an inlet reverberant plenum chamber. The effect of the length of the inlet duct on this sound emission will be investigated by using two different duct lengths.

The effect of the flow variables that are of interest, the relative Mach number and the inlet flow angle, will also be determined. By running the compressor at three speeds and three different discharge valve settings at each speed the effect of these variables on the MPT evolution can be determined.

Experimental Facility

Test Compressor

The compressor consists of a single stage fan with a 40 blade rotor and a 72 blade outlet guide vane. The rotor is scaled to a 6 in. O.D. and operated in a closed-compressor acoustic test loop. A throttling valve on the discharge side of the compressor is used to control the flow rate. Figure 1 shows the typical blade geometry. Freon 12 is used as the working fluid to reduce the running speed at any given Mach number.

MODEL COMPRESSOR ROTOR (40 BLADES)

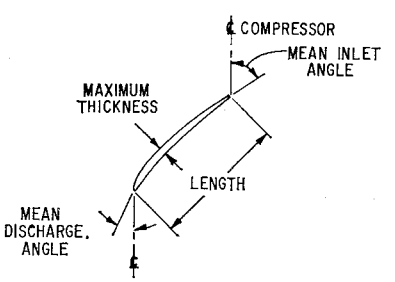

	TIP	PITCH	HUB
RADIUS (IN.)	2.957	2.549	2.196
MAX. THICKNESS (IN.)	0.014	0.020	0.022
LENGTH (IN.)	0.591	0.520	0.445
MEAN INLET ANGLE	63°54'	56°43'	55°56'
MEAN DISCH. ANGLE	57°14'	48°33'	40°26'

Fig. 1 Rotor blade geometry.

Presented as Paper 72-127 at the AIAA 10th Aerospace Sciences Meeting, San Diego, California, January 17–19, 1972; submitted February 10, 1972; revision received June 16, 1972. This paper is based on work performed under Contract No. NASW-1922 for NASA Headquarters, Office of Advanced Research and Technology, Research Division.

Index category: Aircraft Propulsion System Noise.

* Engine Noise Program Engineer.

† Fluid Mechanics Engineer. Member AIAA.

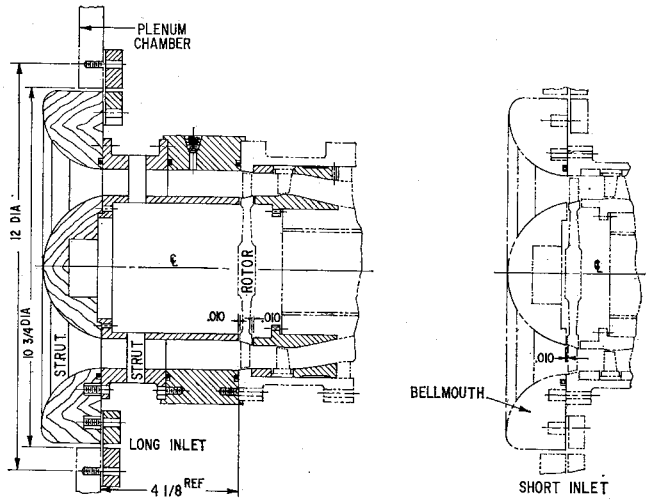

Fig. 2 Compressor layout.

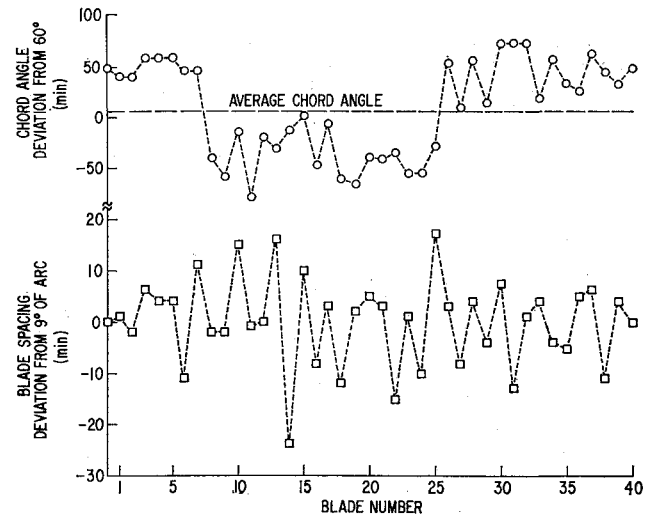

Fig. 3 Rotor nonuniformities.

The compressor inlet section is made of two sections, a constant area annulus and an inlet bellmouth, as seen in Fig. 2. By removing the annular piece the inlet bellmouth can be positioned at the rotor inlet plane. In this manner the effect of the inlet duct length on the inlet noise emission can be studied.

To study the generation of the MPT's, it is helpful to remove all other possible noise sources, if possible. For these tests the inlet guide vanes, IGV's, were removed. The struts in two axial locations (8 in each set), were made very small, 0.047″ thick, and placed as far upstream of the rotor as practical. This will reduce the disruption of the wave pattern to a minimal amount. Also to reduce the noise produced by the rotor wakes impinging on the stator and any potential interaction between the rotor and the stator, the stator is placed about 1.3 rotor blade chords downstream of the rotor.

Acoustic Instrumentation

Inlet wave patterns are measured with piezoelectric pressure transducers manufactured by Kistler Instruments, Model 601L1. These probes are acceleration compensated and have a sensitivity to acceleration of 0.002 psi/g. The probes are mounted so that the sensitive portion is flush with the outer radius of the inlet annulus. These probes are located at 0.77, 2.24 and 3.82 rotor blade spacings ahead of the rotor.

The microphone in the inlet plenum is mounted on a motor driven traversing mechanism that causes an oscillating motion of the microphone, back and forth across the chamber, on a circular arc in a plane not parallel to any of the chamber walls. The path crosses the compressor axis with a radial distance from the compressor inlet to the microphone of approximately 2.5 ft. This motion takes 26 seconds to transverse completely in both directions. The walls of the inlet plenum chamber are hard metal. Hence, with proper calibration and instrumentation it may be used as a reverberation chamber to determine the acoustic power radiated from the compressor inlet. The details of the instruments and calibration technique have previously been described in Ref. 6. Briefly, the procedure is to calibrate the chamber using the "integrated tone-burst method" developed by Schroeder.[7] During compressor tests, measurements were made by a 1/8 in. Bruel and Kjaer Model 4138 condenser microphone which is calibrated in Freon 12 gas using an electrostatic actuator.

Signals from these probes are amplified and fed to a seven channel instrument tape recorder manufactured by the Norelco Corporation. These magnetic tapes are then analyzed in a spectral analyzer, using a 10 Hz bandwidth. This analyzer uses a time-averaging scheme to yield time steady frequency spectrums of the signals. The advantage of this analysis technique is that the time average of the signals is presented and not an instantaneous reading. This reduces the data scatter and produces very clear spectrograms, and is particularly beneficial if the signals have a high random noise content.

Experimental Results and Comparison with Analysis

Inlet Annulus Noise

To obtain a description of the rotor defects, as an input to the analysis described in Ref. 1, the assembled rotor was measured prior to testing. The chord angle and the blade spacing were measured at the tip and are shown on Fig. 3.

Due to the small size of the test rotor, the irregularities are considerably larger than for the full size fan. For example, the maximum stagger angle variation is as much as $\pm 1°$ whereas in the conventional fan, the manufacturing tolerance is usually of the order of $0.5 \sim 0.75$ degrees. The spacing error is much larger than the normal tolerance.

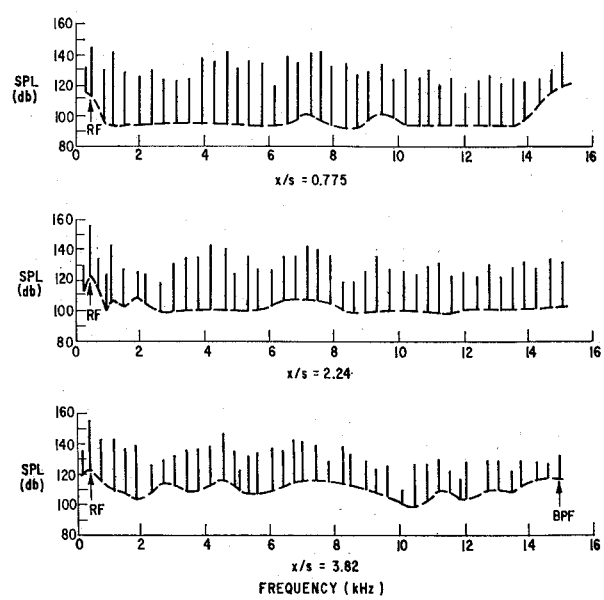

Fig. 4 Inlet annulus SPL spectra ($M_r = 1.26$, $\alpha = 5.1°$).

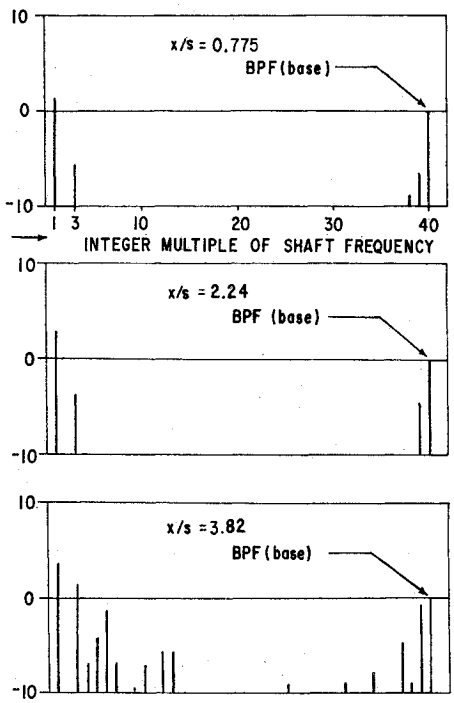

Fig. 5 Computed evolution of MPT for model rotor ($M_r = 1.25$, angle of attack = 1.8°).

A magnetically sensed index mark on the rotor shaft is used as a reference for the blade variation distribution. This variation is then correlated, using an oscilloscope, to the perturbations of the wall static pressure waveforms. Since the pressure wave patterns are helical in nature, it is necessary to extrapolate the tangential position, from the closest transducer position, to the rotor inlet plane. When this is done, a good correlation of the apparent origin of the pressure perturbations and the blade non uniformities is found.

Figure 4 shows the SPL spectrum for the three inlet axial positions. These spectrograms were obtained in the manner indicated previously, using a 10 Hz bandwidth. The vertical lines shown on this figure represent the pure tones and the dashed line is the base of the peaks. It is seen that the largest MPT is at the rotor shaft frequency and the second largest is at the third harmonic.

The computed evolution of MPT is presented in Fig. 5. In the analysis of Ref. 1, it was assumed that shocks are attached at the leading edge. However, in the model fan the leading edges of the blades are quite blunt and the shock is detached. An improvised method is used to handle blunt leading edges. The model blade contour on the suction surface is like a narrow wedge, with a semicircular leading edge. In the computation, it is assumed that the attached shocks start at the transition point between the wedge and the circle. Since this attached shock assumption breaks down for low Mach number, the computation will be limited to the case of higher Mach number. A relative Mach number of 1.25 is used. As for the angle of attack, the restriction that the shocks should be attached at the transition point places some limit on the choice of angle of attack. Here the angle of attack is chosen to be 1.8 degrees, somewhat less than the values at which the experiments were conducted. Only the effects of stagger angle errors and blade spacing errors are included in the calculations, since the limited size of the model fan impeded any precise measurements of the blade contour errors. Thus this effect, which, along with the shock standoff effect, could have potentially significant bearing on the MPT sound, is not included in the computed results. When one compares computed results of Fig. 5 with the measurements, Fig. 4, it is noticed that in the computed results there are virtually no

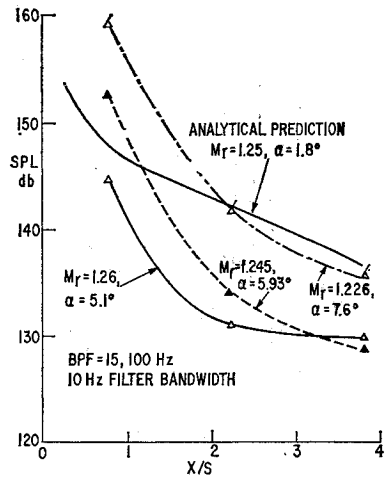

Fig. 6 BPF noise vs axial distance.

MPT's between the tenth and the thirtieth harmonic, whereas in the experimental results there are many MPT's in between. The main reason for this difference is considered to be due to the omission of two aforementioned effects in the analysis. However, the computed results do indicate, in agreement with the experiments that the largest MPT occurs at the rotor shaft frequency and next largest at the third harmonic of the shaft frequency.

The variation of the sound pressure level, SPL, referred to 0.0002 microbar, (contained in a 10 Hz bandwidth around BPF) with upstream axial distance from the rotor is shown on Fig. 6. Figure 7 shows that close to the rotor the BPF noise increases with increasing flow incidence angle. Comparing the predicted values of Fig. 6 with the experimental data, and taking into account the difference of the angle of attack between the measurement and computation, the analysis is seen to overestimate the BPF sound. The discussion of this discrepancy will be given later with regard to Fig. 8.

As can be seen from the previous figures, the BPF noise, decreases rapidly with the upstream axial distance from the rotor, decreases with relative Mach number, in the range of the experiments, and increases with the flow incidence angle. Table 1 shows the effect of other speeds and discharge conditions. One would expect the BPF noise level to be larger due to an increase in the incidence angle, as this will cause the strong shock region of the bow wave to enlarge and penetrate further upstream. The variation with Mach number is also expected since the higher Mach number would be expected to have a faster decay of the BPF content due to faster development of the "skewed" wave patterns. This explanation is somewhat tentative and deserves further investigation.

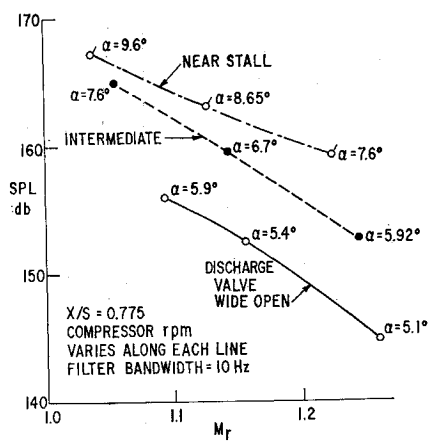

Fig. 7 BPF noise vs relative Mach number.

Table 1 Acoustic summary—long inlet

BPF, kHz	M_r	α deg	X/S	SPL/MRF,[b] db	SPL/MRF, db	SPL/BPF, db
13.25	1.094	5.9	0.775	146.1/3	154.7/20	155.9
			2.24	149.8/1	150.6/19	137.5
			3.82	140.5/3	144.2/19	135.0
13.0	1.057	7.6	0.775	149.9/1	154.6/20	165.9
			2.24	157.4/1	145.2/19	140.3
			3.82	146.7/3	144.4/19	148.4[a]
13.0	1.0375	9.6	0.775	148.5/3	147.8/25	167.2
			2.24	157.8/1	142.7/25	152.4
			3.82	143.3/1	137.2/19	146.9
14.0	1.157	5.4	0.775	149.8/1	155.2/20	152.5
			2.24	158.7/1	150/20	136.4
			3.82	151.3/1	148.3/10	133.1
14.0	1.144	6.7	0.775	151.5/3	157.7/20	159.5
			2.24	166.2/1	155.2/19	136.4
			3.82	152.7/1	153.9/19	136.0
14.0	1.128	8.65	0.775	151.5/3	158.7/15	163.1
			2.24	165.1/1	152.1/19	138.2
			3.82	152.5/1	152.9/15	136.0
15.1	1.26	5.1	0.775	148.8/1	145/12	144.7
			2.24	158.5/1	145.6/11	131.0
			3.82	152.8/1	143.1/12	129.9
15.1	1.245	5.92	0.775	151.3/1	156.2/20	152.6
			2.24	167.1/1	152/20	134.0
			3.82	155.2/1	150.5/20	128.8
15.1	1.226	7.6	0.775	152.6/1	154.6/12	159.2
			2.24	165.8/1	151.7/12	141.8
			3.82	153.3/1	150.7/20	135.5

[a] Broad band noise high.
[b] SPL/MRF—sound pressure level at multiple of rotor frequency (MRF).

The distribution of multiple pure tones is fairly uniform, so that by measuring the maximum peak in the frequency range from 3 to 10 kHz a reasonable measure of the MPT content is obtained. Table 1 shows the SPL at the BPF, at the midrange (MPT) and at the low frequency end (rotor frequency, RF) of the spectrum for all the nine runs. In general, the MPT strength decreases in the upstream direction but not as fast as the BPF noise. Apparently due to the large nonuniformities of the rotor, the prominent MPT's are established very quickly and decay slowly in the upstream direction. This axial decay of the MPT's is in apparent contradiction with previously reported results.[4-5] The reasons for this difference appear to be due to two effects: 1) the level of the MPT's at the first measuring point ($x/s = 0.77$) is large in this study, indicating that the nonuniformities are larger than used previously. This will cause an early establishment of the predominant MPT's. With smaller nonuniformities a larger axial distance is required before the MPT's develop significantly. 2) the previous results indicate that the level of the MPT's reaches a plateau and then travels upstream unchanged. These results, however, are based on measurements taken in an inlet bellmouth which alters the MPT evolution process with respect to what occurs in a constant area annulus.

To show the effect of axial distance on the total spectrum the measured and predicted values of the SPL at the blade passing frequency BPF and the rotor frequency RF are shown in Fig. 8. It is observed that close to the rotor the BPF noise dominates but is soon converted into the dominant rotor frequency noise RF and harmonics of rotor frequency, MPT noise. As mentioned previously in conjunction with Fig. 6, the BPF sound is overpredicted. Here, it is observed that the RF noise is underpredicted. The reasons for this discrepancy in Fig. 8 are diagnosed to be the omission of shock standoff distance and blade contour nonuniformity in the analysis. Both effects would result in the generation of more MPT'S. Thus, the conversion of acoustic energy contained in BPF to MPT sound would be augmented. This tends to decrease the BPF noise while the MPT noise including the RF noise will be increased. In order to assess at least one of the

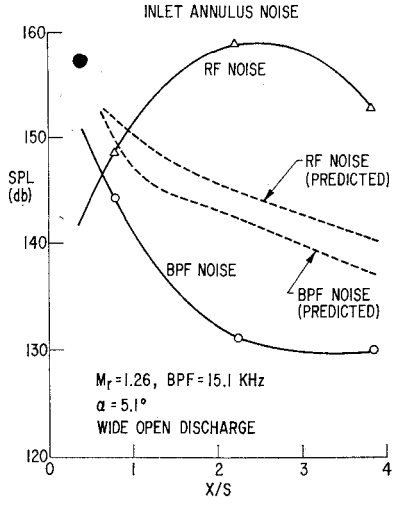

Fig. 8 Inlet BPF noise vs X/S.

two effects quantitatively, the authors recently completed an unpublished study of the effect of shock detachment on the MPT noise. The results of the refined analysis are shown in Fig. 9 along with the corresponding measured values. Agreement between the analysis and the experimental data for the rotor frequency is seen to be markedly improved. Also, agreement for the third harmonic is surprisingly good. This improved prediction of the frequency spectrum shows more MPT's in the intermediate range as compared to Fig. 5 which was computed under attached shock assumption. Thus it more closely resembles the experimental results of Fig. 4. The absolute comparison of the computed and experimental results for the mid-frequency shown in Figure 9 is, however, rather unsatisfactory and this discrepancy could be attributed to the blade contour nonuniformity.

One of the most important parameters in fan design is the rotor Mach number. The influence of Mach number can be seen in Table 1. For a fixed discharge valve setting the MPT

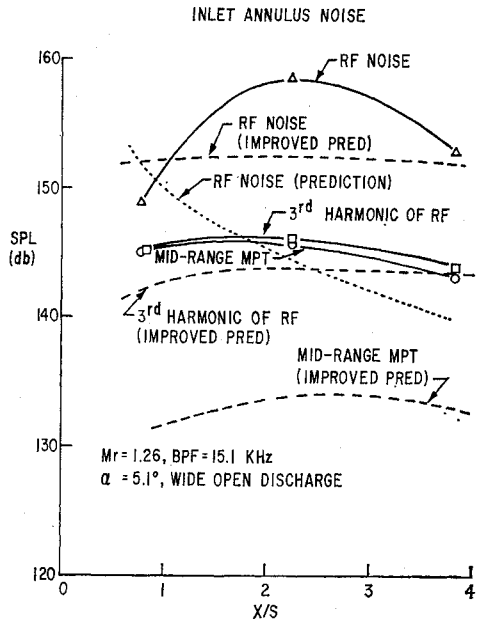

Fig. 9 Inlet MPT noise vs X/S.

noise has a maximum that lies between 1.13 and 1.16, an example of this is seen on Fig. 10. As observed in Fig. 10, above a certain rotor relative Mach number both the MPT noise and the BPF noise decrease with rotor speed. The Mach number range shown here is limited and these trends may change for higher Mach numbers; even so, these trends have important implications to the design of future quiet fan engines.

Short vs Long Inlet Duct (Plenum Noise)

The effect of the inlet duct length on the emitted sound is studied by measuring the sound in the inlet reverberant chamber. While the reverberant chamber used does not provide a measure of the sound directivity, it does give a useful measure of the spatial-averaged sound pressure level. The major effect of removing the long inlet annulus, 4.125 in. in length, and moving the inlet bellmouth to the rotor inlet plane, is to cause a large increase in the over all noise level. The SPL frequency spectra for the long and the short inlet ducts are shown on Fig. 11 and 12, respectively. On Fig. 13, the plenum BP noise is seen to fall rapidly with relative Mach number, like the inlet annulus results, until about $M_r = 1.2$.

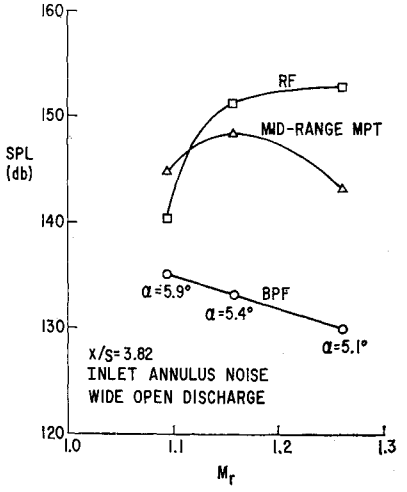

Fig. 10 Inlet Annulus noise vs M_r.

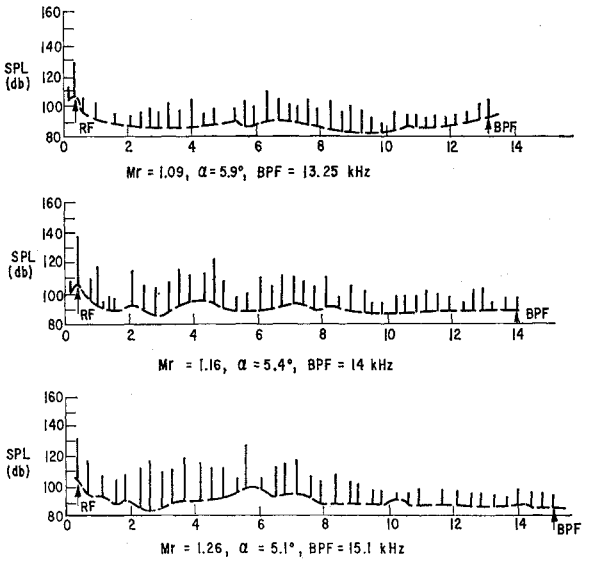

Fig. 11 Plenum SPL spectra (long inlet).

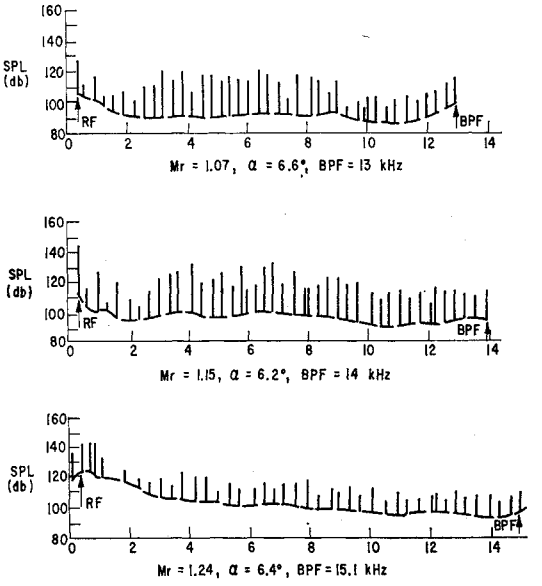

Fig. 12 Plenum SPL spectra (short inlet).

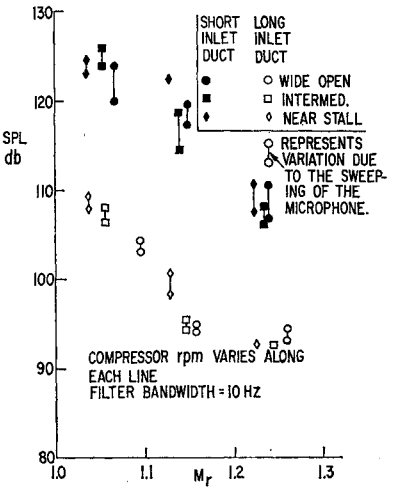

Fig. 13 Plenum BPF vs Mach number.

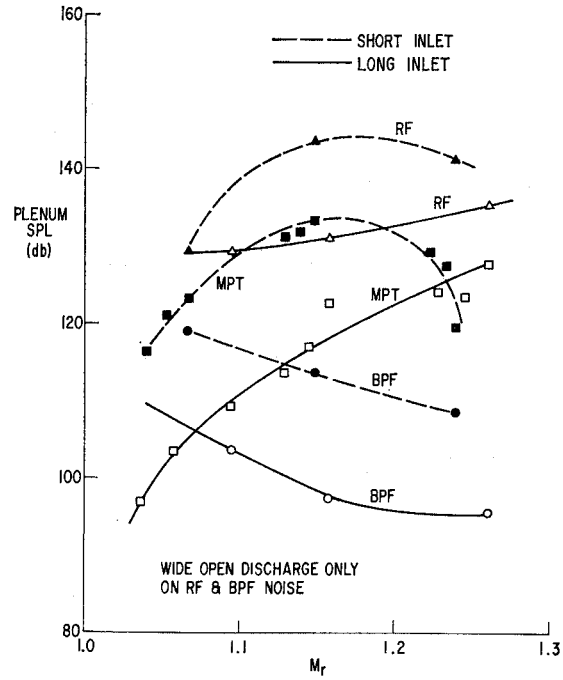

Fig. 14 Plenum noise comparison.

However, the incidence angle variations are seen to have a very much smaller effect on the plenum BPF and also on the MPT noise than on the inlet duct measurements.

The most striking effect shown by the plenum measurements (Fig. 14) is the decrease of the MPT noise with rotor relative Mach number after M_r exceeds 1.15. This trend along with the decrease of the BPF noise with M_r indicates that inlet noise may not limit the application of high Mach number fans. The plenum measurements of long inlet annulus runs, as seen on Fig. 14, have a rising trend with M_r; unfortunately the rotor speed was limited so it could not be determined whether or not the MPF noise would level off and then decline with M_r. These differences in the long and short inlet data do indicate, however, that the length of the inlet duct plays an important role in the level and the spectral content of the emitted noise. Further evidence of this can be seen by comparing the plenum data to the inlet annulus measurements. The plenum MPT's (with the short inlet) have a peak near $M_r = 1.15$ which is very similar to the inlet annulus noise results shown on Fig. 10. This indicates that the short inlet effectively interrupts the midrange MPT evolution process. The transition of the MPT noise from a variation with M_r having a broad maximum to a monotonic increasing function of M_r, as occurred when propagating through the long inlet duct and into the plenum, has not occurred with the short inlet. The abrupt upstream expansion will cause the pressure variations to be greatly diffused and retard the MPT evolution process. This results in different plenum noise spectral shifts with rotor Mach number for the long and short inlet ducts. The clearest differences in the comparable spectra of the long and short inlet cases occur at frequencies above the rotor frequency. The short inlet is seen to have a lower MPT noise content relative to the BPF noise than the long inlet case. In all cases, the noise at the rotor frequency dominates the plenum measurements, with the BPF noise showing up only at the lowest speed runs. Table 2 compares the plenum measurement data with the long and short inlets.

The over all effect of having a short inlet appears to be: 1) a large increase in the rotor frequency noise and BPF noise. 2) an interruption of the MPT noise axial evolution.

Summary

In summary, this study has conducted a combined analytical and experimental program that has demonstrated the following: 1) The MPT sound is due to rotor geometry imperfections, and the angular position of the pressure waveform distortions are correlated to the location of these imperfections. 2) From the analysis based on Ref. 1, the MPT evolution has been computed using the known rotor nonuniformities. The computed result correctly predicts the frequency of the dominant MPT's. 3) Although the absolute sound pressure levels of the BPF and RF sound predicted by the analysis are in the same range as the experimental values, there are considerable discrepancies between them. The cause of this is believed to be the omission of shock standoff distance and blade contour nonuniformity effects in the calculation. A refined analysis, taking the effect of detached shocks into consideration, is found to give much better agreement. 4) Rotor relative Mach number and incidence angle are important parameters to the evolution of the MPT sound. In particular, the measurements indicate that high Mach number fans will have less MPT noise than current high bypass fans. 5) The inlet duct length has an important influence on the sound emission, large enough to suggest that noise control should play a role in inlet design as well as performance considerations.

Table 2 Acoustic summary—plenum

BPF kHz	M_r	α deg	SPL/RF, db	SPL/MRF, db	SPL/BPF, db	
13.25	1.094	5.9	129.3	109.7/19	103.7	
13.0	1.057	7.6	133.9	103.6/19	108.3	
13.0	1.0357	9.6	135.7	97.0/19	109.5	
14.0	1.157	5.4	131.3	122.9/13	97.5	
14.0	1.144	6.7	139.9	117.1/9	97.2	Long inlet
14.0	1.128	8.65	141.1	113.9/14	101.6	
15.1	1.26	5.1	135.7	128.0/16	95.9	
15.1	1.245	5.93	136.0	123.8/10	95.5	
15.1	1.226	7.6	131.5	124.3/10	95.8	
13.0	1.066	6.6	129.5	123.2/20	119.1	
13.0	1.053	8.0	130.8	121.5/15	121.8	
13.0	1.035	9.9	139.6	116.4/12	125.2	
14.0	1.148	6.2	143.8	133.2/20	113.9	
14.0	1.139	7.3	139.5	132.0/12	116.5	Short inlet
14.0	1.129	8.4	146.9	131.3/15	123.3	
15.1	1.239	6.4	141.6	119.9/21	108.7	
15.1	1.233	6.9	144.3	127.8/10	106.7	
15.1	1.222	8.1	148.1	129.3/10	109.6	

References

[1] Kurosaka, M., "A Note on Multiple Pure Tone Noise," *Journal of Sound and Vibration*, Vol. 19, No. 4, Dec. 1971, pp. 453–462.

[2] Kantola, R. A. and Kurosaka, M., "The Theoretical and Experimental Investigations on Multiple Pure Tone Noise," 71-C-315, Nov. 1971, General Electric Co., Corporate Research and Development, Schenectady, N.Y.

[3] Kester, J. D., "Generation and Suppression of Combination Tone Noise from Turbo Fan Engines," *Proceedings AGARD Fluid Dynamics Panel*, Paper 19, 1969.

[4] Sofrin, T. G. and Pickett, G. F., "Multiple Pure Tone Noise Generated by Fans at Supersonic Tip Speed," *International Symposium on the Fluid Mechanics and Design of Turbomachinery*, Pennsylvania State Univ., University Park, Pa. 1970.

[5] Philpot, M. G., "The Buzz-Saw Noise Generated by a High Duty Transonic Compressor," ASME Paper 70-GT-54, May 1970, Brussels, Belgium.

[6] Wells, R. J. and McGraw, J. M., "The Use of Gases Other Than Air in Acoustic Testing of Model Compressors," ASME Paper 67-GT-22. March 1967, Houston, Texas.

[7] Schroeder, M. R., "New Method of Measuring Reverberant Time," *Journal of Acoustical Society of America*, Vol. 37, March 1965, pp. 409–412.

NOVEMBER 1972 J. AIRCRAFT VOL. 9, NO. 11

Design and Test of a Boron/Epoxy Reinforced Airframe

MELVIN J. RICH* and ROBERT T. WELGE†
Sikorsky Aircraft Division of United Aircraft Corporation, Stratford, Conn.

A design investigation is conducted under a NASA contract for stiffening the air frame of the CH-54B Skycrane[R] using boron/epoxy reinforced aluminum stringers. It is shown that the reinforcement will prevent air frame resonance with appreciable weight savings over conventional aluminum construction. Thermal expansion is investigated and not found to be a problem. Tapered joints using a fiber glass insert are investigated and are shown to reduce the adhesive bond load transfer stresses to well within acceptable levels. Static load tests are conducted on reinforced stringers and skin/stringer panels. These tests show that the reinforced stringer has the required stiffness and strength and that while bond strength is the limiting factor, the panel strength in shear and compression exceeds that of the all-aluminum construction. Fatigue tests are conducted for in flight and ground-air-ground vibratory loadings. The results of the fatigue tests are presented and show that the boron/epoxy reinforced stringers meet the required fatigue loadings with a life factor of four. It is concluded that the boron/epoxy reinforced stringers are effective in reducing weight for airframe stiffening, and have more than adequate strength for the structural integrity of the CH-54B.

Introduction

BORON/EPOXY reinforced aluminum stringers offer large weight savings and permit use of conventional fastening. The structural design of large helicopter airframes involves both strength and stiffness. The stiffness requirements arise from the necessity of tuning the air frame to prevent amplification of the rotor vibratory forces. Thus, after providing the strength requirements for flight and ground conditions, it is often necessary to add additional material to increase the natural frequency of the airframe.

The original CH-54 Skycrane airframe, as shown in Fig. 1, was found to be in partial resonance with the main rotor cyclic forces under particular combinations of slung cable length and load. As shown in Fig. 1, the tail cone region was reinforced to increase the vertical bending stiffness. The method of reinforcement, as shown in Fig. 2, was to use thick aluminum skins on the top and bottom of the tail cone shell. This reinforcement added 160 lb to the basic airframe structural weight.

A preliminary analysis showed that bonding uniaxial layers of boron/epoxy strips to 7075-T6 aluminum stringers would save 130 lb and achieve the same stiffness requirements. In addition, as shown in Fig. 3, the use of reinforced aluminum stringers permits a conventional rivet attachment to the aircraft outer skins so that minimum modification and conventional tooling would be required to save the 130 lb in stiffening material.

As a result, a program was conducted under NASA Contract NAS1-10459 to design and evaluate the strength characteristics of the boron/epoxy reinforced stringers for the CH-54B helicopter. This phase of the effort consists of design analysis of the tail cone, developing fabrication techniques, and evaluating static and fatigue strength data.

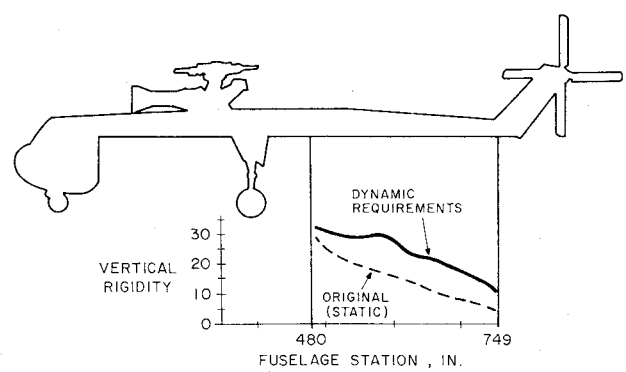

Fig. 1 CH-54 Skycrane Helicopter.

Presented as Paper 72-392 at the AIAA/ASME/SAE 13th Structures, Structural Dynamics, and Materials Conference, San Antonio, Texas, April 10–12, 1972; submitted April 18, 1972; revision received August 21, 1972.

Index categories: Aircraft Structural Materials; Structure-Composite Materials (Including Coatings); VTOL Aircraft Dal sign.

* Chief, Structures Technology. Associate Fellow AIAA.
† Supervisor, Advanced Concepts.